

Controlling selectivity in alkene oxidation: anion driven epoxidation or dihydroxylation catalysed by [Iron(III)(Pyridine-Containing Ligand)] complexes

Giorgio Tseberlidis,^a Luca Demonti,^a Valentina Pirovano,^b Marco Scavini,^a Serena Cappelli,^a Silvia Rizzato,^a Rubén Vicente^c and Alessandro Caselli^{a*}

^a Department of Chemistry and ISTM-CNR-Milano, Università degli Studi di Milano, via Golgi 19 – 20133 Milano, Italy. Email: alessandro.caselli@unimi.it

^b Department of Pharmaceutical Sciences, General and Organic Chemistry Section “A. Marchesini”, University of Milan, Via Venezian 21 – 20133, Milano, Italy.

^c Departamento de Química Orgánica e Inorgánica, and Instituto Universitario de Química Organometálica “Enrique Moles”, Universidad de Oviedo. c/ Julián Clavería 8, 33007, Oviedo, Spain. Email: vicenteruben@uniovi.es.

ABSTRACT:

A highly reactive and selective catalytic system comprising Fe(III) and macrocyclic pyridine-containing ligands (Pc-L) for alkene oxidation by using hydrogen peroxide is reported herein. Four new stable iron(III) complexes have been isolated and characterized. Importantly, depending on the anion of the iron(III) metal complex employed as catalyst, a completely reversed selectivity was observed. When X = OTf, a selective dihydroxylation reaction took place. On the other hand, employing X = Cl resulted in the epoxide as the major product. The reaction proved to be quite general, tolerating aromatic and aliphatic alkenes as well as internal or terminal double bonds and both epoxides and diol products were obtained in good yields with good to excellent selectivities (up to 93% isolated yield and *d.r.* = 99:1). The catalytic system proved its robustness by performing several catalytic cycles, without observing catalyst deactivation. The use of acetone as a solvent and hydrogen peroxide as terminal oxidant renders this catalytic system appealing.

INTRODUCTION

Iron, the most abundant transition metal on earth, and its complexes are knowing an increasing interest in organic synthesis.^[1] The reasons why homogeneous iron catalysis has become a focal research area after the turn of the millennium are brilliantly explained by Fürstner in a recent Outlook.^[2] In particular, the field of iron-catalysed oxidation reactions is of great importance not only in synthetic organic chemistry, but also in biochemistry and industrial applications. As a result,^[3] the research in this area had an impressive boost, as witnessed by several timely reviews.^[4] Synthetic chemists have developed nonheme iron based systems that are capable of mimicking the high efficiency in selective oxidation of non-activated substrates possessed by natural metalloenzymes (mono- and di-oxygenases).^[5] Despite these efforts, and the exponential growing number of scientific papers appeared since 1960 to now, artificial catalyst systems that can compete with Nature are still challenging.^[6] In order to design catalysts capable of performing high regio- and/or stereo-selective C-H or C=C bond oxidations, it is important the choice of critical components of iron coordination sphere, namely the donor atoms and their geometry. Moreover, the need for sustainability imposes a strict control of the reaction conditions and the choice of the oxidant in this respect is of fundamental importance to assure the green principles of the overall process. In terms of atom-economy and E-factor,^[7] dioxygen, O₂, and hydrogen peroxide, H₂O₂, are by far the reagents of choice since they possess the highest oxygen content.^[8] From a synthetic point of view, however, the usage of H₂O₂ seems to be more favourable since it is easier to handle, whilst molecular oxygen is always associated with potential risk of explosion and very often requires the presence of a stoichiometric organic sacrificial coreductant.^[9] With hydrogen peroxide, instead, water is the only by-product formed.

Amongst nonheme catalysts, iron complexes of polyamine and aminopyridine ligands are the most used.^[10] In particular, iron(II) complexes of tetradentate N₄ donor-ligands have proven to act as efficient homogeneous catalysts in epoxidation^[11] or *syn*-dihydroxylation^[12] of alkenes with aqueous hydrogen peroxide as terminal oxidant.

In the past few years, we have reported the synthesis of a series of pyridine-based 12-membered tetraaza-macrocyclic ligands (Pc-L)^[13] and the application of their copper(I)^[14] and silver(I)^[15] complexes in catalysis. Spurred by the very recent reports on the generation of a highly reactive iron species by reaction of peracetic acid with a ferrous complex ([Fe^{II}(CF₃SO₃)₂(PyNMe₃)], Figure 1a),^[16] we became interested in exploring the coordination properties of our Pc-L ligands with iron. We report herein that robust ferric complexes can indeed be obtained in excellent yields and that these complexes are competent catalysts for alkene oxidation by aqueous hydrogen peroxide even in the absence of any additives (Figure 1b). Remarkably, we observed a dependency on the reaction outcome with respect to the anion employed for the synthesis of the iron(III) metal complex. Thus, when X =

OTf, a selective alkene dihydroxylation reaction occurred. On the other hand, employing X = Cl, alkene epoxidation was the preferred product.

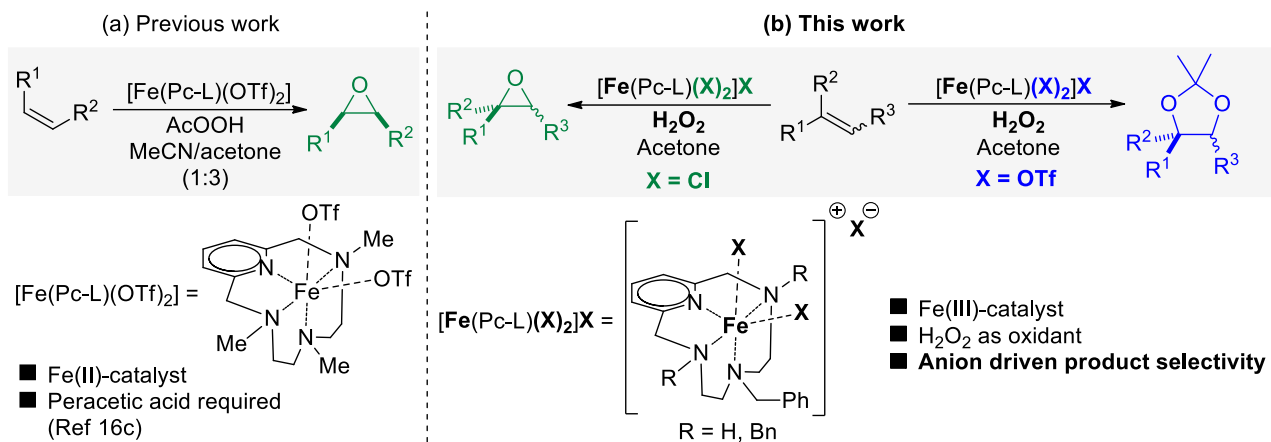
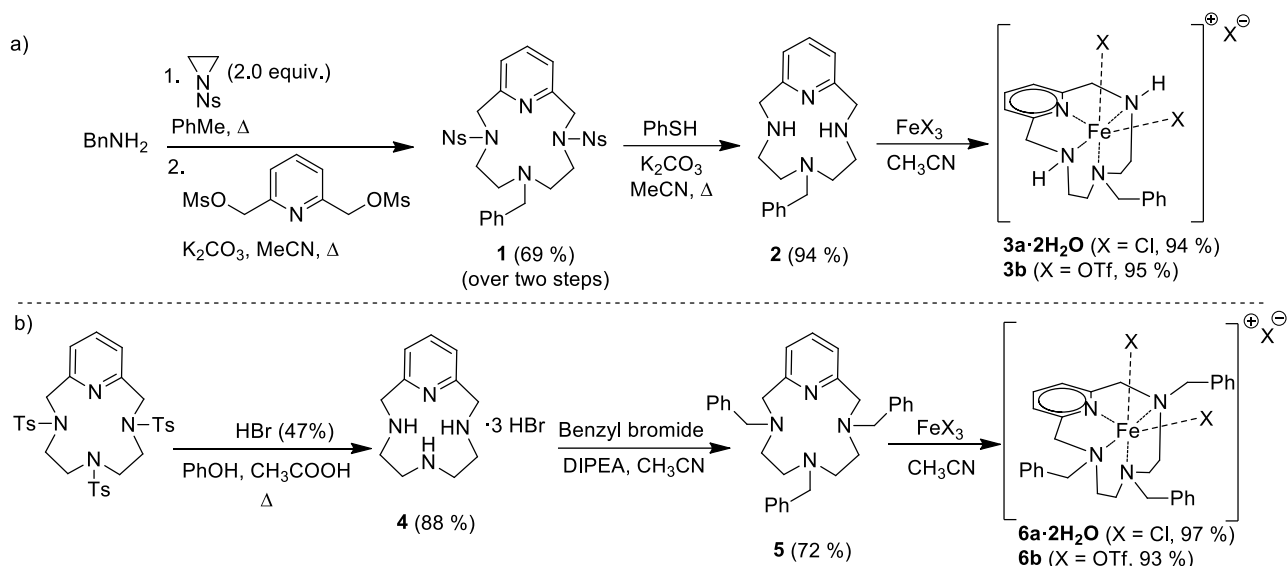


Figure 1. a) OAT reaction catalysed by ferrous complex [Fe^{II}(CF₃SO₃)₂(PyNMe₃)] reported by Serrano-Plana and others; b) controllable epoxidation or dihydroxylation reactions catalysed by ferric complex reported in this work.

RESULTS AND DISCUSSION

Preparation of the iron complexes. The selected pyridine-based 12-membered tetraaza macrocyclic Pc-L **2** was obtained in useful overall yield by a modified Richman-Atkins procedure according to Scheme 1a. We found that for this particular ligand, almost quantitative yields were obtained by the mild hydrolysis of *ortho*-nosyl (Ns) protecting groups of ligand **1** (see Supporting Information for details). On the other hand, macrocycle **5** could be easily synthesized by treatment of an *N*-tritosyl-diethylenetriamine with pyridine-2,6-diylbis(methylene) dimethanesulfonate, in the presence of K₂CO₃ as a base under heterogeneous conditions.^[16c] After the hydrolysis in HBr of the Ts protecting groups, the bromohydrated salt **4** has been directly perbenzylated in the presence of excess of DIPEA (DIPEA = *N,N*-diisopropylethylamine) as a base (Scheme 1b).



Scheme 1. Synthetic route used to obtain ligands **2** and **5** and their corresponding ferric complexes **3** and **6**. Ns= *ortho*-nosyl, DIPEA = *N,N*-diisopropylethylamine.

We choose Fe(III) as preferred metal for the oxidation of alkenes due to its well known great activity towards the generation of metal-oxo complexes and related oxygen transfer reactions.^[17]

The complexes were obtained by treating an acetonitrile solution of the selected ligand with an acetonitrile solution of aqueous iron(III) chloride or iron(III) triflate salts at room temperature in a 1:1 ligand to metal ratio, although the triflate complexes could be prepared conveniently by anion exchange from complex **6a·2H₂O** and silver triflate as well (see Supporting Information).^[18] The structures of complexes **3a-b** and **6a-b** have been characterized by means of mass and elemental analysis as detailed in the Supporting Information. Elemental analyses for the iron chloride complexes **3a·2H₂O** and **6a·2H₂O** are consistent with the presence of two molecules of water. Based on the ionization observed, together with literature data, we propose for the metal complexes the structure depicted in Scheme 1, with the iron placed in an octahedral environment and only two X groups directly bound to the metal (X = Cl or OTf). Magnetic moments, μ_{eff} , of 3.73 μ_{B} and of 3.88 μ_{B} were measured by the Evans' method for complexes **6a·2H₂O** and **6b**, respectively. These room temperature magnetic moments are in agreement with a mixture low spin and high spin sites.^[19]

In order to have a better characterization of the spin state of the complexes we decided to perform EPR experiments on **6a·2H₂O** and **6b** complexes in powder form. Figure 2a shows the EPR spectrum of **6a·2H₂O** collected at RT (black curve). Beside a broad asymmetric line around $g \approx 2.06$ (line centred at ≈ 3312 Gauss, $\Delta H_{\text{pp}} \approx 300$ Gauss), a tiny one appear around $g \approx 4.38$, corresponding to 1560 Gauss (see inset, Figure 2a). Moving to 77 K (red curve), the intense resonance peak increases its anisotropy turning into an axial g tensor with the perpendicular g_{\perp} components around ≈ 2.120

(≈ 3215 G) and the parallel $g_{\parallel} \approx 1.77$ (≈ 3850 G). The broad ($\Delta H_{pp} \approx 370$ Gauss) low field feature grows in intensity in respect to RT.

Tang *et al.* observed similar features in $\{[\text{Fe}(\text{mph})_2](\text{ClO}_4)(\text{MeOH})_{0.5}\}_2$ at 149 K and attributed them to rhombic high spin ($g=4.69$, $S=5/2$) and low spin ($g=2.06$, $S=1/2$) Fe^{3+} contributions.^[20] Peak broadening of the latter peak was related to spin-spin interaction. Differently from figure 2a, the intensity of the low field feature decreased on decreasing T.

EPR spectra of complex **6b** (see Figure 2b) shows absorption phenomena at low field and in the 3000-4000 G zone, with several differences in respect to the previous sample. First of all the low field line seems to be more intense than in **6a**·**2H₂O** and more structured with a broad component with $g \approx 7.75$ around 880 Gauss and an intense peak at $g \approx 4.32$ (≈ 1575 G, $\Delta H_{pp} \approx 170$ Gauss). Their positions do not change on cooling, while their intensities increase and the $g=4.32$ component sharpens ($\Delta H_{pp} \approx 85$ Gauss). In the high field region a broad bump is followed by a low intensity peak around $g \approx 2.07$ (≈ 3290 G), that seems to be almost unaffected by temperature (see inset of Figure 2b). Brewer *et al.* observed almost identical spectra in Fe(III) coordination compounds and attributed the absorption phenomena to a dominant transition arising from $m_s = \pm 1/2$ doublet of a Fe^{3+} $S=5/2$ spin state with nearly axial symmetry coupled to a component originated from the $m_s = \pm 3/2$ doublet in the same spin/charge state.^[21]

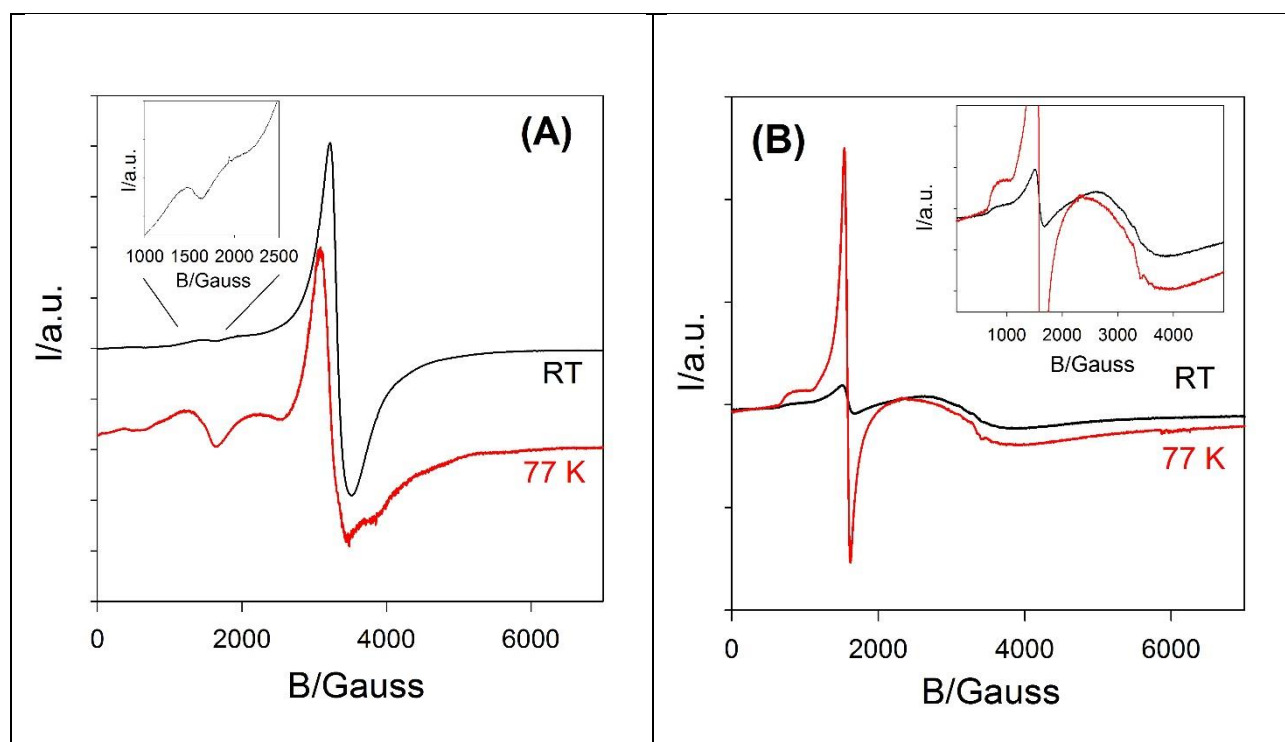


Figure 2. a) EPR spectra for complex **6a**·**2H₂O** collected at RT (black curve) and 77 K (red curve), the inset highlights the signal at RT in the 1000-2500 Gauss interval; b) EPR spectra for complex **6b** collected at RT (black curve) and 77 K (red curve), the inset highlights the signal in the 100-4900 Gauss interval.

Summarizing, in **6a**·2H₂O both low (S=1/2) and high (S=5/2) spin Fe³⁺ species are present. Lowering *T* the intensities related to the S=5/2 state grow up suggesting that it should be the ground electronic state of iron. In **6b** only S=5/2 phenomena appear at both temperature. Moreover, the slow field signals of **6b** are sharper than the ones for **6a**·2H₂O, suggesting some interatomic spin-spin relaxation phenomena in the latter sample as a consequence of reduced average Fe-Fe distance.

Unfortunately, all attempts to grow crystals suitable for X-ray structural determination of the iron complexes meet with failure. However, we discovered that by changing the molar ratio between ligand **5** and the iron chloride source to 1:2 in the synthesis of the metal complex, a new species characterized as ([Fe^{III}(Cl)₂(³BnPc-L)](FeCl₄), **6a'**, could be obtained. Single crystals suitable for X-Ray crystallography were grown by slow evaporation from acetone/ether solution (Figure 3).

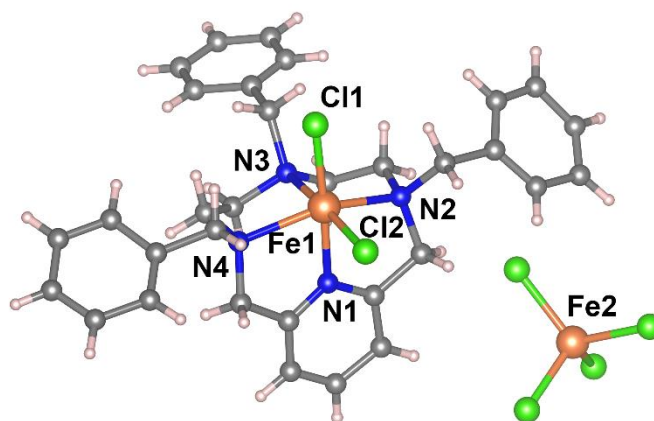


Figure 3. Molecular structure of the complex **6a'** with (FeCl₄)⁻ as counteranion. The acetone solvent is omitted for clarity. Selected bond lengths (Å): Fe(1)-N(1) 2.102(14), Fe(1)-N(2) 2.231(14), Fe(1)-N(3) 2.285(15), Fe(1)-N(4) 2.223(13), Fe(1)-Cl(1) 2.234(5), Fe(1)-Cl(2) 2.278(6). Full crystal structure data of **6a'**·(ace) are reported in the Supporting Information.

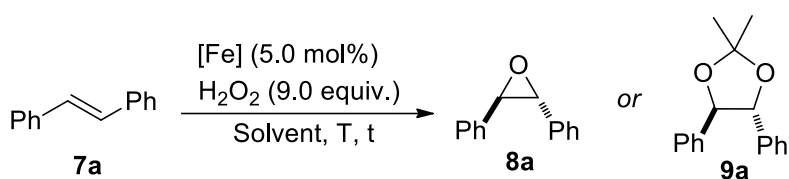
In the complex **6a'** the iron(III) exhibits a largely *distorted octahedral* geometry (see caption figure 3 and table S3). The coordination sphere consist of four N-donors from the tetra-azamacrocyclic, which adopts the expected *cis*-folded configuration, and two *cis* chloride ions. The pyridine ring is responsible for the large deviation from linearity of the axial N(2)-Fe(1)-N(4) bond angle that is comparable to the values found in the literature for complexes containing analogous cyclic chelators.^[21-22] Other structural parameters, such as Fe-N bond distances, are similar to those reported for related systems.^{[21][23]} The equatorial Fe(1)-N(1) (pyridine nitrogen) bond is the shortest and thus the strongest metal-ligand bond, although all Fe-N bond lengths are longer than 2.0 Å, typical of high-spin Fe(III)-complexes.^[24]

Iron-catalyzed alkene oxidations. At the outset, oxidation of *trans*-stilbene **7a** by H₂O₂ served as benchmark for the optimization of the reaction conditions (**Table 1**). The reaction proceeded well using acetone, in presence of 5 mol% of **3a·2H₂O**, at 30 °C leading to *trans* epoxide **8a** with almost full conversion and a remarkable 95% of selectivity in 48 h (entry 1, **Table 1**). Higher temperatures (60 °C) resulted in a faster reaction but in a loss of selectivity (77%, entry 2, **Table 1**). The use of acetonitrile provided full conversion yet lower selectivity compared to acetone (entry 3, **Table 1**). On the other hand, branched alcohols, known for being suitable solvents often used in oxidations, showed good selectivities but with poor conversions (entries 4-5, **Table 1**). In other commonly used reaction media, the reaction did not take place (entries 6-8, **Table 1**).

When we moved to complex **6a·2H₂O**, we were pleased to find that even higher selectivities in epoxide formation could be obtained (entry 9, **Table 1**). This is most probably due to the better solubility of complex **6a·2H₂O** in the reaction medium. Moreover, with this catalyst, higher temperatures were allowed together with a decrease in the excess of oxidant used (6 instead of 9 equiv.), and the *trans* epoxide was selectively formed in 24 h (95% selectivity, 99% conversion, entry 10, **Table 1**). A lower catalyst loading of 1 mol% resulted in lower conversion and selectivity (entry 11, **Table 1**). The rest of the reaction mass balance is represented by benzaldehyde (10% selectivity) and traces of 2-phenylacetophenone.

Remarkably, when triflate iron complexes were used as catalysts under otherwise identical reaction conditions, we observed a different reaction outcome. Indeed, by using iron(III) complex **3b**, acetal **9a**, arising from the corresponding dihydroxylation product derived from *trans*-stilbene was obtained with 65% of selectivity (*trans/cis* ratio 5:1, epoxide was not detected, while benzaldehyde accounted for the rest of the mass balance, entry 12, **Table 1**). Using iron(III) complex **6b**, the selectivity was improved and product **9a** was isolated in 86% yield, confirming the data for conversion and selectivities obtained by GC analysis with internal standard (entry 13, **Table 1**). The ¹H NMR spectrum confirmed the correct assignment of the major isomer as *trans*.

The crucial role of the ligand was further demonstrated since iron(III) triflate, as well as iron(III) chloride in the absence of any ligand, did not provide any oxidation product, under otherwise identical reaction conditions after 5 days (entry 14, **Table 1**).

Table 1. Optimization of $[\text{Fe}^{\text{III}}(\text{X})_2(\text{Pc-L})]\text{X}$ catalysed alkene oxidation^a

Entry	Catalyst	Solvent	Temp	Time	Epoxide (8a) %	Acetal (9a) %
					Select (conv) ^b	Select (conv) ^b
1		acetone	30 °C	48h	95 (97)	-
2		acetone	60 °C	36h	77 (95)	-
3		CH ₃ CN	30 °C	48h	75 (99)	-
4	3a·2H₂O	<i>t</i> -BuOH	60 °C	48h	96 (45)	-
5		<i>t</i> -amylOH	30 °C	48h	88 (32)	-
6		TFE	30 °C	48h	-	-
7		H ₂ O	30 °C	48h	-	-
8		PhCl	30 °C	48h	-	-
9		acetone	30 °C	48h	97 (95)	-
10 ^c	6a·2H₂O	acetone	60 °C	24h	95 (99)	-
11 ^d		acetone	60 °C	24h	85 (58)	-
12 ^c	3b	acetone	60 °C	48h	-	65 (99)
13 ^c	6b	acetone	60 °C	24h	-	87 (99) ^e
14 ^f	Fe(X)₃	acetone	60 °C	5 days	-	traces
15 ^{c,g}	6b	acetone	60 °C	24h	34	60 (83)

^a Reactions were performed with $[\text{Fe}^{\text{III}}]$ (2.5×10^{-2} mmol) in the solvent (10 mL) at a cat/stilbene/ H_2O_2 ratio of 1:20:180; H_2O_2 (30% sol) was added in three portions every 12 h. ^b Conversions and selectivities were calculated by GC (dodecane as internal standard). ^c cat/stilbene/ H_2O_2 ratio of 1:20:120; H_2O_2 (30% sol) was added in two portions every 12 h. ^d cat/stilbene/ H_2O_2 ratio of 1:100:600. ^e Isolated in 86% yield as a mixture of *trans* and *cis* acetonide in 5:1 ratio. ^f X = Cl or Tf. ^g BHT (2.5×10^{-2} mmol) was added to the reaction mixture.

Dihydroxylation versus epoxidation. Epoxides can be readily converted into acetonides in the presence of catalytic amounts of Lewis acids in acetone as solvent.^[25] Among the catalysts used, both $\text{Fe}(\text{OTf})_3$ ^[26] and anhydrous FeCl_3 ^[27] salts were reported to promote this reaction with good yields.

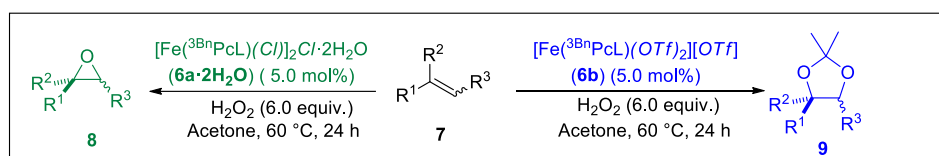
On the other hand, it is well known that strong acids can readily open epoxides. Hintermann and co-workers have elegantly shown that HOTf generated from metal triflate precursors can indeed act as a hidden Brønsted acid catalyst.^[28] Treatment of the isolated epoxide **8a** in the presence of catalytic amounts of triflic acid in acetone with H₂O₂ yielded to the corresponding acetal, **9a** (*trans/cis* ratio 4:1.), in 8 hours, as expected, the same results can be obtained employing complex **6b** instead of HOTf (see Supporting Information). It is reasonable to assume that, under our reaction conditions, hidden HOTf might act as a non-innocent species in the epoxide ring opening (as well as in the acetal formation). It should be noticed that, to the best of our knowledge, the possible role of hidden Brønsted acid catalysis in dihydroxylation reactions promoted by FeL_n(OTf)_m complexes reaction has not been investigated in previous reports.

On the other hand, it is commonly accepted in literature that tetradentate iron complexes with *cis*-labile coordination sites allows for a facile formation of a Fe(III)-hydroperoxo species in situ and the mechanism of the catalytic O-O cleavage has been the object of several studies.^{[4a,b][6a][29]} It has been reported that there is a correlation between the iron spin state in octahedral Fe(III) hydroperoxo complexes of tetradentate ligands in *cis* geometry^[30] and the epoxide/diol ratio provided in alkene oxidation. Low-spin complexes (S = 1/2) tend to be epoxide selective, while high spin complexes lead mainly to diols. In particular, product distribution can be controlled by modification of the ligand steric properties or complex geometry.^[31] As demonstrated by our EPR analysis (see above) changing the counteranion from chloride to triflate causes an increase of high spin population of the iron metal centre. Thus, these analyses provide a rationale for the exquisite product selectivity observed. Anyway, a possible role also of complex **6b** and/or hidden triflic acid in the opening of the epoxide cannot be completely ruled out at the present stage (see Supporting Information).

Scope of the alkene oxidations. With these preliminary studies in our hands, we decided to study the scope of the reaction by using catalysts **6a·2H₂O** and **6b** (**Table 2**). The catalytic system was found to tolerate a wide range of substrates. When using complex **6a·2H₂O**, the reaction proceeds with excellent yields and selectivities for internal tri- and disubstituted aromatic alkenes (**Table 2**, products **8a,b,c**). A preference towards the formation of *trans* products was observed (determined by GC-MS and NMR analysis, see Supporting Information), even starting from *cis* substrates (**Table 2**, product **8a**). A similar result was reported also when using FeCl₃·6H₂O in the presence of 1-methylimidazole using hydrogen peroxide as terminal oxidant.^[32] Starting from *trans*-stilbene, the observed *trans/cis* epoxide ratio was 99:1, while starting from *cis*-stilbene *trans/cis* epoxide ratio was 9:1. Since a radical mechanism can be proposed to explain this results, we have run two additional test reactions by using catalysts **6a·2H₂O** and **6b** under the optimized reaction conditions in the presence of BHT (BHT = dibutylhydroxytoluene) as radical trap (see Supporting Information). In

both cases, we observed a lower conversion, although the reaction is not completely inhibited. More interestingly, also the diol/epoxide ratio is influenced by the presence of the radical trap, in particular when employing complex **6b** as catalyst, where **9a** is obtained in 60% selectivity, accompanied by the formation of epoxide **8a** (34%), which is never observed in the standard reaction conditions (entry 15, Table 1).

Table 2. Scope of alkene oxidations catalysed by complexes **6a·2H₂O** and **6b^a**



Results expressed in: Selectivity (conversion; *d.r.*)

Alkene	with 6a	with 6b	Alkene	with 6a	with 6b	Alkene	with 6a	with 6b
	 95% (99%)	 86% (99%; 4:1)		 (n.d.)	 76% (99%; 2:1) with 6b 80% (99%; 2:1) with 6a		 79% (99%; 1.3:1)	 83% (99%)
	99% (81%; 9:1)	80% (60%; 4:1)		 (n.d.)	 63% (99%) with 6b 78% (99%) with 6a		 99% (33%)	 85% (25%; 1.6:1)
	 95% (79%; 5:1)	 91% (99%; 4:1)		 54% (99%)	 36% (99%)		 98% (73%)	 99% (50%)
	 80% (99%)	 81% (99%)		 61% (99%)	 41% (99%)		 20% (95%)	 64% (75%)
	 (n.d.)	 99% (99%) with 6b 93% (99%) with 6a		 n.d. (99%)	 26% (99%)		 35% (78%; 4:1)	 99% (31%)

^a Reactions were performed with [Fe^{III}] (2.5 × 10⁻² mmol) in acetone (10 mL) at a cat/stilbene/H₂O₂ ratio of 1:20:120. H₂O₂ (30% sol) was added in two portions every 12 h. Conversions and selectivities were calculated by GC and GC-MS (dodecane as internal standard, n.d. = not detected). ^b *trans* diastereoisomer was obtained as major product. Isolated in 93% yield for **8a**, 75% for **8b**, 85% yield for **9a** and 90% for **9b** (relative stereochemistry of the substituents shown). ^c Obtained as a mixture of the acetonide and the non-protected diol (see Supporting Information for details). ^d **9m** was also detected with a 22% selectivity (*d.r.* = 9:1). ^e Only one diastereoisomer was observed, no traces of the acetonide were detected. ^f **9n** was also detected with a 50% selectivity as a mixture of four diastereoisomer in relative ratio 26:4:1:1. ^g Only two diastereoisomers were observed in 9:1 relative ratio, no traces of the acetonide were detected.

Electron-poor styrenes showed complete conversions but the epoxide was obtained with moderate selectivities (Table 2, products **8g,h**). In both cases formation of other oxidation products such as the

aldehyde and the acetophenone were observed. On the other hand, electron donating substituents on the aromatic ring are not well tolerated and, for example, 4-methoxystyrene was completely converted but in a number of different oxidation products (**Table 2**, product **8i**). Other terminal styrenes, β -methylstyrene and indene underwent the ring opening of the formed epoxide, which was not detected, to yield a mixture of the acetonide and the unprotected diol (**Table 2**, products **9d,e,f,j'**). A lower control of the diastereoselectivity in those case was observed and, for example, diol **9j'** was obtained with *d.r.* = 1:1.3. More challenging substrates such as methyl cinnamate, despite the modest conversion, gave excellent results in terms of product and diastereoselectivity (**Table 2**, product **8k**, only *trans* isomer was detected).

Aliphatic alkenes worked well with this catalytic system. 1-Octene reacted to provide the corresponding epoxide in almost quantitative selectivity and very good yield (**Table 2**, product **8l**). On the other hand, cyclohexene produced the corresponding epoxide **8m** with only 20% of selectivity, accompanied by the diol **9m** (22%; *d.r.* = 9:1) (**Table 2**, product **8m**). The rest of the yield was attributed to the plethora of oxidation products of cyclohexene, amongst which the major product formed was 2-cyclohexene-1-one (33%). This result is the evidence of a preference to diol formation starting from endocyclic substrates and was confirmed performing the reaction on limonene, where, together with epoxide **8n** (35%), the corresponding diol **9n** was formed as main product with 50% selectivity (**Table 2**, product **8n**). A complete regioselectivity towards the oxidation of the internal double bond over the terminal one was observed and, more interestingly, a quite good stereocontrol was observed. In fact, the *trans*-epoxide was obtained in a 4-fold excess with respect to the *cis* and out of the four possible diastereoisomers that could be obtained upon ring opening, a 26:4:1:1 ratio was determined by GC-MS analysis.

By exchanging the counter anion from chloride to triflate, using **6b**, the reaction outcome was reverted providing the acetonide as the main reaction product (**Table 2**, right columns). In few cases, traces of the corresponding non-protected diols were also detected by GC-MS (see Supporting Information for details). The two products are both the result of a dihydroxylation reaction, and for this reason, selectivities are given as the sum of the two products.

The reaction proceeds with excellent yields and selectivities for most of the tested unbiased styrene derivatives (**Table 2**, products **9a,b,c,d,e,f,j**) and shows a preference towards the formation of *trans* products, even starting from *cis* substrates, exactly like in the epoxidations previously reported. This result is in contrast to what observed in the Fe(III) catalysed conversion of epoxides to acetonide,^[27] where diastereoisomeric mixtures of acetonides were obtained starting from pure *trans*-epoxides. It is worth to note that, when employing complex **6b** the acetonide **9j** was obtained major compound

and a single diastereoisomer has been detected by GC-MS, in contrast to what observed in the case of the reaction catalysed by complex **6a**·2H₂O, where both diastereoisomers of **9j'** diol were formed. Electron-poor styrenes as well as more electron-rich ones were tolerated but showed lower selectivities (**Table 2**, products **9g,h,i**), while cinnamate, gave quite good results in terms of selectivity (although with no stereocontrol, *d.r.* = 1.2:1), but a low conversion (**Table 2**, product **9k**). Even with aliphatic substrates the reaction proceeded well, giving excellent selectivity in the case of 1-octene (**Table 2**, product **9l**) and reasonable results for cyclohexene and limonene (**Table 2**, products **9m,n**). Again, in the case of limonene, a complete regioselectivity for the internal double bond over the terminal one was observed. More interestingly, a single diastereoisomer was obtained for **9m** and out of the four possible diastereoisomers only two, in 9:1 ratio, were observed for **9n**. The robustness of the catalytic system was proved by performing repeated batches of the benchmark reaction simply by adding the reagents after each cycle ends, avoiding the isolation of the metal complex. Thus, with catalyst **6a**·2H₂O an isolated yield of 90% (TON = 54) of three cycles was obtained (95% one single batch, GC yield). Similarly, catalyst **6b** provided 84% (TON = 84) isolated yield after five cycles (86% one single batch, GC yield). It should be noticed that product (and by-product) accumulation generated along the consecutive cycles had a minor impact in catalyst deactivation, which is stable and productive even after five days of reaction.

Conclusions

In summary, we have demonstrated that both epoxidation and dihydroxylation of terminal and internal alkenes can be efficiently and selectively achieved by using a catalytic system comprising Fe(III) and pyridine-containing ligands (Pc-L). This catalytic system takes advantage of an economic metal source and an easy to assemble macrocyclic ligand. Remarkably, a complete reversal of selectivity between the epoxide and the dihydroxylation product could be induced by the proper choice of the anion. A rationale for this selectivity might be the influence of the counteranion in the spin state of iron. The possible role of hidden HOTf in the opening of the epoxide cannot be ruled out when iron triflate complexes are used (due to the presence of water in the reaction media). The use of acetone as a solvent and of hydrogen peroxide as terminal oxidant are appealing features when considering green-chemistry. Studies directed towards a better understanding of the mechanism and a more efficient ligand design to address the problem of stereocontrol of the C-O bond formed are currently undergoing in our laboratories.

EXPERIMENTAL SECTION

General experimental details. All of the reactions that involved the use of reagents sensitive to oxygen or hydrolysis were carried out under an inert atmosphere. The glassware was previously dried

in an oven at 110 °C and was set with cycles of vacuum and nitrogen. All chemicals and solvents were commercially available and were used as given except where specified. The chromatographic column separations were performed by a flash technique, using silica gel (pore size 60 Å, particle size 230–400 mesh, Merck grade 9385) or by gravimetric technique using basic Al₂O₃. For TLC, silica was used on TLC Alu foils with fluorescent indicator (254 nm) and the detection was performed by irradiation with UV light ($\lambda = 254$ nm or 366 nm). ¹H NMR analyses were performed with 300 or 400 MHz spectrometers at room temperature. The coupling constants (*J*) are expressed in hertz (Hz), and the chemical shifts (δ) in ppm. ¹³C NMR analyses were performed with the same instruments at 75.5, and 100 MHz, and attached proton test (APT) sequence was used to distinguish the methine and methyl carbon signals from those arising from methylene and quaternary carbon atoms. All ¹³C NMR spectra were recorded with complete proton decoupling. The ¹H NMR signals of the ligand described in the following have been attributed by correlation spectroscopy (COSY) and nuclear Overhauser effect spectroscopy (NOESY) techniques. Assignments of the resonance in ¹³C NMR were made using the APT pulse sequence and heteronuclear single quantum correlation (HSQC) and heteronuclear multiple bond correlation (HMBC) techniques. EPR measurements were performed on powder samples with a Bruker ELEXSYS spectrometer equipped with an ER4102ST standard regular cavity at X band (9.55 GHz) frequency at room temperature and at 77 K using a cold finger Quartz Dewar cooled by liquid nitrogen, The derivative dP/dH of power *P* adsorbed was recorded as a function of the static magnetic field *H*. Low resolution MS spectra were recorded with instruments equipped with electron ionization (EI), ESI/ion trap (using a syringe pump device to directly inject sample solutions), or fast atom bombardment (FAB) (for Pc-L and metal complexes) sources. The values are expressed as mass–charge ratio and the relative intensities of the most significant peaks are shown in brackets. Gas chromatographic analyses were performed with GC-FAST technique using a Shimadzu GC-2010 equipped with a Supelco SLBTM-5ms capillary column. GC-MS analyses were performed using a ISQTM QD Single Quadrupole GC-MS (Thermo Fisher) equipped with a VF-5ms (30 m x 0.25 mm i.d. x 0.25 μ m; Agilent Technology). Elemental analyses and ICP-OES were recorded in the analytical laboratories of Università degli Studi di Milano. X-ray data collection for the crystal structure determination was carried out by using Bruker Smart APEX II CCD diffractometer with the Mo K radiation ($\lambda = 0.71073$) at 296 K. Synthesis of the ligands and iron complexes is described in the experimental section.

General procedure for the synthesis of Fe(III) complexes.

A solution of FeCl₃·6H₂O or Fe(OTf)₃ (0.36 mmol) in acetonitrile (4.0 mL) was added dropwise to a solution of ligand **2** or **5** (0.36 mmol) in acetonitrile (4.0 mL). The mixture was left to react for 60 minutes at room temperature showing a change of color from orange to dark brown. The solvent was

then evaporated in vacuum and the crude was treated with Et₂O (5 mL) and left under stirring at room temperature for 30 minutes. The product obtained as dark brown solid was then filtered and dried in vacuum.

Yields	3a·2H₂O	94% [iron source: FeCl ₃ ·6H ₂ O]
	MS (FAB)	m/z (%) 422 (100), 424 (63) [M-Cl]
	Elem. An.	C ₁₈ H ₂₈ Cl ₃ FeN ₄ O ₂ Calcd: C 43.71; H 5.71; N 11.33; Found: C 43.81; H 5.49; N 11.47
	3b	95% [iron source: Fe(OTf) ₃ anhydrous]
	MS (FAB)	m/z (%) 501 (100), 503 (27) [M-2OTf]
	Elem. An.	C ₂₁ H ₂₄ F ₉ FeN ₄ O ₉ S ₃ Calcd: C 31.55; H 3.03; N 7.01; Found: C 32.01; H 3.24; N 7.49
	6a·2H₂O	97% [iron source: FeCl ₃ ·6H ₂ O]
	MS (FAB)	m/z (%) 567 (100), 569 (62) [M-2Cl]
	Elem. An.	C ₃₂ H ₄₀ Cl ₃ FeN ₄ O ₂ Calcd: C 56.95; H 5.37; N 8.30; Found: C 56.83; H 5.73; N 8.08
	6b	93% [iron source: Fe(OTf) ₃ anhydrous]
	MS (FAB)	m/z (%) 830 (100), 831 (37) [M-OTf]
	Elem. An.	C ₃₅ H ₃₆ F ₉ FeN ₄ O ₉ S ₃ Calcd: C 42.91; H 3.70; N 5.72; Found: C 42.34; H 4.04; N 6.08

General catalytic procedure

The catalyst (0.025 mmol), the substrate (0.5 mmol) and dodecane (60 μL, used as GC internal standard) were dissolved in acetone (10.0 mL). H₂O₂ 30% (1.5 mmol) was added and the mixture was heated for 10 hours at 60 °C. Then H₂O₂ 30% (1.5 mmol) was added and the mixture was heated for further 12-14 hours. After this period the catalyst was removed by filtration on celite pad and a sample of the so-obtained crude (*c* = 0.1 mg/mL) was used for GC and GC-MS analyses.

ASSOCIATED CONTENT

Supporting Information

Detailed experimental procedures, text, figures and tables reporting full NMR spectra for all ligands and characterization of the iron complexes. EPR data for complexes **6a·2H₂O** and **6b**. General catalytic procedures and procedures employed for the isolation of selected reaction products, including figure and tables reporting full NMR characterization. GC methods used and GC-MS spectra for all the catalytic run reported, and ¹H NMR of selected reaction crudes. X-Ray data for complex **6a'**. Tables containing the results of the cost evaluation studies. This material is available free of charge via the Internet

ACKNOWLEDGEMENT

Financial support from the Università degli Studi di Milano "Unimi – piano di sostegno alla ricerca 2015-17 – Linea 2 Azione B " and from Ministerio de Economía y Competitividad (MINECO), Agencia Estatal de Investigación (AEI) and Fondo Europeo de Desarrollo Regional (FEDER) (CTQ2016-76840-R) is gratefully acknowledged. A. C. and G. T. are grateful to Nicola Panza for precious help in the synthesis of ligand **4**, and to Dr. Matteo Compagnoni for his advices and help in performing a cost evaluation study. M.S. gratefully thanks Prof. Cesare Oliva for useful discussions.

KEYWORDS

Dihydroxylation; Epoxidation; Macrocycles; Nonheme iron complexes; Pyridine containing macrocyclic ligands.

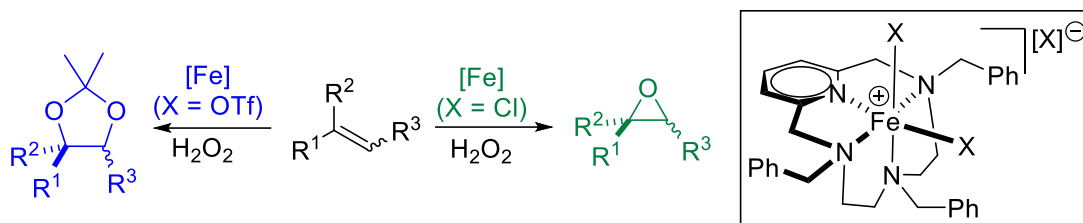
REFERENCES

- [1] I. Bauer, H.-J. Knölker, *Chem. Rev.* **2015**, *115*, 3170-3387.
- [2] A. Furstner, *ACS Cent Sci* **2016**, *2*, 778-789.
- [3] C. Bolm, J. Legros, J. Le Paih, L. Zani, *Chem. Rev.* **2004**, *104*, 6217-6254.
- [4] a) S. M. Hoelzl, P. J. Altmann, J. W. Kueck, F. E. Kuehn, *Coord. Chem. Rev.* **2017**, *352*, 517-536; b) I. Gamba, Z. Codola, J. Lloret-Fillol, M. Costas, *Coord. Chem. Rev.* **2017**, *334*, 2-24; c) K. Gopalaiah, *Chem. Rev.* **2013**, *113*, 3248-3296; d) T. Wai-Shan, G. Q. Chen, Y. Liu, C. Y. Zhou, C. M. Che, *Pure Appl. Chem.* **2012**, *84*, 1685-1704; e) E. P. Talsi, K. P. Bryliakov, *Coord. Chem. Rev.* **2012**, *256*, 1418-1434; f) M. Costas, *Coord. Chem. Rev.* **2011**, *255*, 2912-2932; g) B. B. Eike, *Curr. Org. Chem.* **2008**, *12*, 1341-1369; h) S. Enthaler, K. Junge, M. Beller, *Angew. Chem. Int. Ed.* **2008**, *47*, 3317-3321; i) A. Correa, O. Garcia Mancheno, C. Bolm, *Chem. Soc. Rev.* **2008**, *37*, 1108-1117; j) W. Nam, *Acc. Chem. Res.* **2007**, *40*, 522-531; k) E. Rose, B. Andriolletti, S. Zrig, M. Quelquejeu-Etheve, *Chem. Soc. Rev.* **2005**, *34*, 573-583.
- [5] a) L. Vicens, M. Costas, *Dalton Trans.* **2018**, *47*, 1755-1763; b) O. Cusso, M. W. Giuliano, X. Ribas, S. J. Miller, M. Costas, *Chem. Sci.* **2017**, *8*, 3660-3667; c) G. Olivo, O. Cusso, M. Borrell, M. Costas, *JBIC, J. Biol. Inorg. Chem.* **2017**, *22*, 425-452; d) G. Olivo, O. Cusso, M. Costas, *Chem. - Asian J.* **2016**, *11*, 3148-3158; e) L. Que, W. B. Tolman, *Nature* **2008**, *455*, 333-340; f) S. V. Kryatov, E. V. Rybak-Akimova, S. Schindler, *Chem. Rev.* **2005**, *105*, 2175-2226.
- [6] a) W. N. Oloo, L. Que, *Acc. Chem. Res.* **2015**, *48*, 2612-2621; b) A. Fingerhut, O. V. Serdyuk, S. B. Tsogoeva, *Green Chem.* **2015**, *17*, 2042-2058; c) S. P. de Visser, J.-U. Rohde, Y.-M. Lee, J. Cho, W. Nam, *Coord. Chem. Rev.* **2013**, *257*, 381-393.
- [7] R. A. Sheldon, *Chem. Soc. Rev.* **2012**, *41*, 1437-1451.
- [8] a) G. Strukul, A. Scarso, in *Liquid Phase Oxidation Via Heterogeneous Catalysis: Organic Synthesis and Industrial Applications* (Eds.: M. G. Clerici, O. A. Kholdeeva), **2013**, pp. 1-20; b) J. Piera, J. E. Bäckvall, *Angew. Chem. Int. Ed.* **2008**, *47*, 3506-3523.
- [9] K. P. Bryliakov, *Chem. Rev.* **2017**, *117*, 11406-11459.
- [10] a) K. P. Bryliakov, E. P. Talsi, *Coord. Chem. Rev.* **2014**, *276*, 73-96; b) C.-L. Sun, B.-J. Li, Z.-J. Shi, *Chem. Rev.* **2011**, *111*, 1293-1314.
- [11] a) O. Cusso, J. Serrano-Plana, M. Costas, *ACS Catal.* **2017**, *7*, 5046-5053; b) O. Cusso, M. Cianfanelli, X. Ribas, R. J. M. Klein Gebbink, M. Costas, *J. Am. Chem. Soc.* **2016**, *138*, 2732-2738; c) O. Cussó, X. Ribas, J. Lloret-Fillol, M. Costas, *Angew. Chem. Int. Ed.* **2015**, *54*, 2729-2733; d) O. Cussó, I. Garcia-Bosch, X. Ribas, J. Lloret-Fillol, M. Costas, *J. Am. Chem. Soc.* **2013**, *135*, 14871-14878; e) X. Wang, C. Miao, S. Wang, C. Xia, W. Sun, *ChemCatChem* **2013**, *5*, 2489-2494; f) B. Wang, S. Wang, C. Xia, W. Sun, *Chem. Eur. J.* **2012**, *18*, 7332-7335; g) O. Y. Lyakin, R. V. Ottenbacher, K. P. Bryliakov, E. P. Talsi, *ACS Catal.* **2012**, *2*, 1196-1202; h) E. A. Mikhalyova, O. V. Makhlynets, T. D. Palluccio, A. S. Filatov, E. V. Rybak-Akimova, *Chem. Commun.* **2012**, *48*, 687-689; i) W. Ye, D. M. Ho, S. Friedle, T. D. Palluccio, E. V. Rybak-Akimova, *Inorg. Chem.* **2012**, *51*, 5006-5021; j) F. Odon,

- E. Girgenti, C. Lebrun, C. Marchi-Delapierre, J. Pécaut, S. Ménage, *Eur. J. Inorg. Chem.* **2012**, 2012, 85-96; k) M. Wu, C. X. Miao, S. Wang, X. Hu, C. Xia, F. E. Kühn, W. Sun, *Adv. Synth. Catal.* **2011**, 353, 3014-3022; l) R. Mas-Ballesté, L. Que, *J. Am. Chem. Soc.* **2007**, 129, 15964-15972; m) M. C. White, A. G. Doyle, E. N. Jacobsen, *J. Am. Chem. Soc.* **2001**, 123, 7194-7195.
- [12] a) M. Borrell, M. Costas, *J. Am. Chem. Soc.* **2017**, 139, 12821-12829; b) C. Zang, Y. Liu, Z. J. Xu, C. W. Tse, X. Guan, J. Wei, J. S. Huang, C. M. Che, *Angew. Chem. Int. Ed.* **2016**, 55, 10253-10257; c) I. Prat, D. Font, A. Company, K. Junge, X. Ribas, M. Beller, M. Costas, *Adv. Synth. Catal.* **2013**, 355, 947-956; d) T. W.-S. Chow, E. L.-M. Wong, Z. Guo, Y. Liu, J.-S. Huang, C.-M. Che, *J. Am. Chem. Soc.* **2010**, 132, 13229-13239; e) R. Mas-Balleste, M. Fujita, J. L. Que, *Dalton Trans.* **2008**, 1828-1830; f) J. Y. Ryu, J. Kim, M. Costas, K. Chen, W. Nam, L. Que Jr, *Chem. Commun.* **2002**, 1288-1289.
- [13] G. Tseberlidis, D. Intriери, A. Caselli, *Eur. J. Inorg. Chem.* **2017**, 2017, 3589-3603.
- [14] a) V. Pirovano, E. Brambilla, G. Tseberlidis, *Org. Lett.* **2018**, 20, 405-408; b) G. Tseberlidis, A. Caselli, R. Vicente, *J. Organomet. Chem.* **2017**, 835, 1-5; c) B. Castano, E. Gallo, D. J. Cole-Hamilton, V. Dal Santo, R. Psaro, A. Caselli, *Green Chem.* **2014**, 16, 3202-3209; d) B. Castano, S. Guidone, E. Gallo, F. Ragaini, N. Casati, P. Macchi, M. Sisti, A. Caselli, *Dalton Trans.* **2013**, 42, 2451-2462; e) B. Castano, P. Zardi, Y. C. Honemann, A. Galarneau, E. Gallo, R. Psaro, A. Caselli, V. Dal Santo, *RSC Adv.* **2013**, 3, 22199-22205; f) B. Castano, T. Pedrazzini, M. Sisti, E. Gallo, F. Ragaini, N. Casati, A. Caselli, *Appl. Organomet. Chem.* **2011**, 25, 824-829; g) A. Caselli, F. Cesana, E. Gallo, N. Casati, P. Macchi, M. Sisti, G. Celentano, S. Cenini, *Dalton Trans.* **2008**, 4202-4205.
- [15] a) G. Tseberlidis, M. Dell'Acqua, D. Valcarengi, E. Gallo, E. Rossi, G. Abbiati, A. Caselli, *RSC Adv.* **2016**, 6, 97404-97419; b) T. Pedrazzini, P. Pirovano, M. Dell'Acqua, F. Ragaini, P. Illiano, P. Macchi, G. Abbiati, A. Caselli, *Eur. J. Inorg. Chem.* **2015**, 2015, 5089-5098; c) M. Dell'Acqua, B. Castano, C. Cecchini, T. Pedrazzini, V. Pirovano, E. Rossi, A. Caselli, G. Abbiati, *J. Org. Chem.* **2014**, 79, 3494-3505; d) M. Trose, M. Dell'Acqua, T. Pedrazzini, V. Pirovano, E. Gallo, E. Rossi, A. Caselli, G. Abbiati, *J. Org. Chem.* **2014**, 79, 7311-7320.
- [16] a) R. Fan, J. Serrano-Plana, W. N. Oloo, A. Draksharapu, E. Delgado-Pinar, A. Company, V. Martin-Diaconescu, M. Borrell, J. Lloret-Fillol, E. Garcia-Espana, Y. Guo, E. L. Bominaar, L. Que, Jr., M. Costas, E. Munck, *J. Am. Chem. Soc.* **2018**, 140, 3916-3928; b) J. Serrano-Plana, F. Acuna-Pares, V. Dantignana, W. N. Oloo, E. Castillo, A. Draksharapu, C. J. Whiteoak, V. Martin-Diaconescu, M. G. Basallote, J. M. Luis, L. Que, Jr., M. Costas, A. Company, *Chemistry* **2018**, 24, 5331-5340; c) J. Serrano-Plana, A. Aguinaco, R. Belda, E. García-España, M. G. Basallote, A. Company, M. Costas, *Angew. Chem. Int. Ed.* **2016**, 55, 6310-6314; d) J. Serrano-Plana, W. N. Oloo, L. Acosta-Rueda, K. K. Meier, B. Verdejo, E. García-España, M. G. Basallote, E. Münck, L. Que, A. Company, M. Costas, *J. Am. Chem. Soc.* **2015**, 137, 15833-15842.
- [17] a) B. Bitterlich, K. Schröder, M. K. Tse, M. Beller, *Eur. J. Org. Chem.* **2008**, 2008, 4867-4870; b) F. G. Gelalcha, G. Anilkumar, M. K. Tse, A. Brückner, M. Beller, *Chem. Eur. J.* **2008**, 14, 7687-7698.
- [18] After careful analysis of the EPR spectra and ICP-OES data, we found in fact that commercial iron triflate purchased by us contains traces of Mn (around 0.1% with respect to iron). Since it is well known that manganese complexes are also able to catalyze oxidations of alkenes, we choose to use in our catalytic test the iron complex **6b** prepared by anion exchange reaction from **6a**·2H₂O that does not contain manganese (see Supporting Information).
- [19] M. D. Timken, D. N. Hendrickson, E. Sinn, *Inorg. Chem.* **1985**, 24, 3947-3955.
- [20] J. Tang, J. Sánchez Costa, S. Smulders, G. Molnár, A. Bousseksou, S. J. Teat, Y. Li, G. A. van Albada, P. Gamez, J. Reedijk, *Inorg. Chem.* **2009**, 48, 2128-2135.
- [21] S. M. Brewer, P. M. Palacios, H. M. Johnston, B. S. Pierce, K. N. Green, *Inorg. Chim. Acta* **2018**, 478, 139-147.
- [22] H. M. Johnston, P. M. Palacios, B. S. Pierce, K. N. Green, *J. Coord. Chem.* **2016**, 69, 1979-1989.
- [23] a) N. W. Alcock, D. H. Busch and C. Y. Liu, CSD Commun., 2007, CCDC 639154; b) N. W. Alcock, D. H. Busch and C. Y. Liu, CSD Commun., 2007, CCDC 639153.
- [24] R. Shannon, *Acta Crystallographica Section A* **1976**, 32, 751-767.
- [25] A. Solladié-Cavallo, E. Choucair, M. Balaz, P. Lupattelli, C. Bonini, N. Di Blasio, *Eur. J. Org. Chem.* **2006**, 2006, 3007-3011.
- [26] N. Iranpoor, H. Adibi, *Bulletin of the Chemical Society of Japan* **2000**, 73, 675-680.
- [27] S. Saha, S. K. Mandal, S. C. Roy, *Tetrahedron Lett.* **2008**, 49, 5928-5930.
- [28] T. T. Dang, F. Boeck, L. Hintermann, *J. Org. Chem.* **2011**, 76, 9353-9361.

- [29] a) B. Wang, Y.-M. Lee, M. Clémancey, M. S. Seo, R. Sarangi, J.-M. Latour, W. Nam, *J. Am. Chem. Soc.* **2016**, *138*, 2426-2436; b) H. Hirao, N. Thellamurege, X. Zhang, *Front Chem* **2014**, *2*, 14-14.
- [30] M. Fujita, M. Costas, L. Que, *J. Am. Chem. Soc.* **2003**, *125*, 9912-9913.
- [31] K. Chen, M. Costas, J. Kim, A. K. Tipton, L. Que, *J. Am. Chem. Soc.* **2002**, *124*, 3026-3035.
- [32] K. Hasan, N. Brown, C. M. Kozak, *Green Chem.* **2011**, *13*, 1230-1237.

GRAPHICAL ABSTRACT



Controllable iron(III)-catalysed alkene epoxidation or dihydroxylation reactions are performed by judicious choice of anion in [Fe(III)(Pc-L)] catalysts (Pc-L = pyridine-based 12-membered tetraaza-macrocyclic ligands). The catalytic system proved its robustness by performing several catalytic cycles, without observing catalyst deactivation. The use of acetone as a solvent and hydrogen peroxide as terminal oxidant renders this catalytic system appealing.